Design of Microprocessor-Based System for Positioning Servomechanism with Induction Motor

Milić R. Stojić and Slobodan N. Vukosavić

Abstract—**In this paper, digital control algorithms are proposed for the position-controlled system with the inverter-fed induction motor. Two structures of positioning servomechanism are suggested in which the appropriate digital control laws are applied and the straightforward method for adjusting of controller parameters is developed. The method enables the designer to match the desired dynamic performance and to eliminate the steady-state position error due to the presence of a constant or a slowly varying load disturbance. Particular attention is paid to the nonlinear position control design, which preserves the desired response even in the case when electrical torque reaches limits imposed by the inverter current capacity. To illustrate the proposed design procedure and to verify the efficiency of the nonlinear control laws, the simulation results and waveforms from an experimental setup are presented.**

I. Introduction

HIGH-PERFORMANCE servo drives are required in many applications of digitally controlled machines. The usual choice for these applications was the dc motor, since its torque and flux are controlled independently, through two separate terminals. Although the induction motor has superior peak torque capability, acceleration characteristics, power density, and reliability over the dc motor, it was not applied in high-performance servo drives until the vector-control concept, fast semiconductor power switches, and high-speed microcontrollers were introduced. As it is known [1], [2], the vector control enables the induction motor flux and torque to be controlled independently; thus, the induction motor reveals control characteristics of dc motor.

The decoupled induction motor can be employed as the actuator in positioning servomechanisms. When the torque response time is compared with time constants inside the mechanical portion of the control system, it may be assumed to be instantaneous [3]. The maximum electrical torque is usually limited by the inverter current capacity; thus, when the appropriate controller structure and parameter setting are selected, the vector-controlled induction motor may be treated as a proportional gain block with the symmetrical limit. For the position control, Lin and Tsai [4] proposed the variable structure approach. The introduction of the sliding mode operation reconciles the conflict between requirements for the steady-state accuracy and the fast and well-damped response, but it also brings out the pulsating character of the electrical torque inherent to the sliding mode. Haneda and Nagao [5] proposed parameter setting based on the minimization of the conventional quadratic performance index. The position control often requires aperiodical step response of the maximum speed as well as the robustness with respect to load torque disturbances. Recall that these requirements cannot be related with the quadratic performance index in a straightforward way.

This paper presents the method of selecting the appropriate system structure and control parameters for the microprocessor-based positioning servomechanism with the induction motor. The proposed design procedure guarantees the maximum speed of the system aperiodical step response even in the case of imposed constraints such as the bounded accessible shaft speed and the limited available electrical torque.

In Section II, two different structures for position-controlled drive with the induction motor are proposed. The first structure comprising P and D action is applied when a constant or slowly varying load torque disturbance could be neglected. In the presence of constant or slowly varying load torque disturbances, the second structure for control system is suggested. This structure comprises P, I, and D actions appropriately located and arranged so as to match the desired system step response and to eliminate the steady-state position error. For both aforementioned structures, the design procedures are given, enabling the control parameters setting to be performed in a straightforward manner.

The positioning servomechanism with linear controllers, applied in the first and second structures, enters the nonlinear mode of operation for large disturbances due to the shaft speed and electrical torque limitation of the real system. To preserve the desired transient response, we suggest suitable modifications of proposed position controllers. The modification consists in the application of nonlinear control laws introduced in order to obtain the aperiodical step response with maximum speed in the case of a large position set point where the saturation in the electrical torque occurs. The discussion concerning nonlinear control laws includes also the comparison of the proposed nearly time-optimal nonlinear position control with the one obtained by limiting the slope of the position reference and/or by subjecting the reference signal of the local speed control loop to magnitude constraints.

Manuscript received January 25, 1990; revised February 18, 1991.

M. R. Stojić is with the Electrical Engineering Faculty, University of Belgrade, Belgrade, Yugoslavia.

S. N. Vukosavić is with the Electrical Engineering Institute Nikola Tesla, Belgrade, Yugoslavia.

IEEE Log Number 9102180.

0278-0046/91/1000-0369$01.00

For the sake of brevity, only a brief review of some results and literature related to vector control of induction motor are given in Section III, emphasizing the mechanism for compensation of rotor resistance fluctuations. The adaptation mechanism developed in this paper is well suited for the position-controlled induction motor. Thus, Section III comprises necessary information related to the experimental setup.

A detailed performance analysis of the proposed control systems based on results obtained in an experimental setup through the data acquisition/monitor system is given in Section IV. The paper ends with some comments and concluding remarks in Section V.

II. Regulators for Position Control

The torque response time of the vector-controlled induction motor equipped with the appropriate switching algorithm for fast stator current control [6] may be neglected when compared to the time constant of mechanical portion of the position system. Thus, the generated electrical torque may be considered proportional to the torque command representing the system control variable. On the other hand, in a real positioning mechanism with ac motor, limitation factors as the bounded current capacity (or limited available torque), and the limited resolution of the counting-type incremental encoder detecting shaft position must be taken into account. Consequently, a proper structure of control system will depend on system nonlinearities as well as upon the nature of the load torque disturbances $T_L(t)$. In the following, two different control structures are suggested.

A. PD Regulator for Position Control

Fig. 1 shows the system structure with digital PD controller, which compensates an undesired dynamic inside the system plant. To avoid sudden changes in the control variable m and the electrical torque $T_e = K_m m$ when the position set point is changed, the reference signal is included only in the P action, whereas the D action is replaced from the main loop into the local minor loop of the system.

In the linear regime of operation, the z transforms of the system output $\Theta_0(z)$ and control variable $U(z)$ can be easily derived [7]:

$$\Theta_0(z) = \frac{K_m T^2}{2J}\frac{z+1}{(z-1)^2}U(z) - \frac{T^2}{2J}\frac{z+1}{(z-1)^2}T_L^*(z) \tag{1}$$

$$U(z) = K_p K_n^*[\Theta_r(z) - \Theta_0(z)] - K_d K_n^*(1-z^{-1})\Theta_0(z) \tag{2}$$

where K_m is the gain factor of the electrical torque, J is the moment of inertia, T is the sampling period, K_n^* is number of pulses per radian of the incremental encoder; and K_p and K_d denote P and D gain factors, respectively. For the sake of simplicity, instead of the load torque $T_L(t)$, the signal $T_L^*(t)$ representing the samples of the $T_L(t)$ averaged within the sampling periods is introduced in (1). It is convenient to

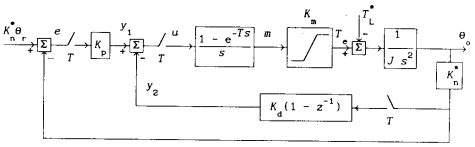

Fig. 1. Block diagram of the position servo with PD controller.

define the synthetic parameter

$$C = \frac{K_m K_n^* T^2}{2J} \tag{3}$$

Then the closed-loop system transfer functions with respect to position reference angle $\Theta_r(t)$ and the torque disturbance $T_L(t)$ are derived respectively as

$$\frac{\Theta_0(z)}{\Theta_r(z)} = \frac{CK_p(z+1)L}{F_1(z)} \tag{4}$$

and

$$\frac{\Theta_0(z)}{T_L^*(z)} = \frac{T^2}{2J}\frac{z(z+1)}{f_1(z)} \tag{5}$$

where $F_1(z)$ represents the closed-loop system characteristic polynomial

$$f_1(z) = z^3 + (CK_p + CK_d - 2)z^2 + (1 + CK_p)z - CK_d. \tag{6}$$

When the system is stable, and in the presence of step changes in the reference angle $\theta_r(t) = \theta_r h(t)$ and in the torque disturbance $T_L(t) = T_L h(t)$, the steady-state value $\theta_0(\infty)$ of the output angle can be calculated by using (4)-(6) to obtain

$$\theta_0(\infty) = \left((1-z^{-1})\Theta_0(z)\right)_{z=1} = \theta_r - \frac{T^2}{2J}\frac{1}{CK_p}T_L. \tag{7}$$

From (7) we conclude that the steady-state position error $e_{ss} = \theta_r(\infty) - \theta_0(\infty)$ depends only on the magnitude of a constant load disturbance; thus, the proposed structure in Fig. 1 may be applied when this magnitude is negligible.

On the other hand, (7) shows that the steady-state accuracy is greatly affected by the sampling time T, which is, for this reason, to be selected small. However, the permissible sampling rate is bounded because of noises due to a finite switching frequency of the inverter, associated torque ripples, and quantization error caused by the counting-type incremental encoder measuring the output angle. To estimate the proper sampling time, the real positioning servomechanism with the induction motor and the encoder having resolution of 1/2500 was simulated for sampling time of 1, 3, and 10 ms. The simulation results (see Fig. 2) show that the torque exhibits an unacceptable "chattering" if the sampling time is lower than 10 ms; therefore, we adopt $T = 10$ ms.

In many applications (lifts and robot servos, for example) it is desired to obtain the aperiodical step response with settling time as small as possible. In such a case, the position

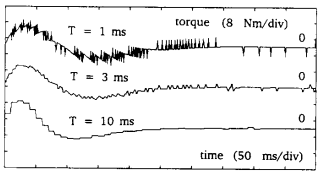

Fig. 2. Torque responses for different sampling periods.

error will not change the sign, and therefore optimal values of the controller parameters K_p and K_d may be determined by minimizing the performance index

$$\mathcal{J} = \sum_{k=0}^{\infty} e(kT). \tag{8}$$

From the system block diagram in Fig. 1, the error $E(z)$ with respect to the step input $\Theta_r(z) = \theta_r/(1 - z^{-1})$ is derived as

$$E(z) = \frac{z[L(z-1) + CK_d(z+1)]}{f_1(z)}\theta_r. \tag{9}$$

Then the performance index (8) can be calculated as

$$\mathcal{J} = E(z)|_{z=1} = \frac{2CK_d}{f_1(1)}\theta_r = \frac{K_d}{K_p}\theta_r. \tag{10}$$

Hence, the setting of the controller parameters is reduced to the problem of determining the minimal value of K_d/K_p under the constraint that all closed-loop system poles are to be real, positive, and inside the unit circle of the z plane. Let us assume the system closed-loop poles to be σ_1, σ_2, and σ_3. Then, according to (6), we have

$$\sigma_1\sigma_2\sigma_3 = CK_d \tag{11a}$$

$$\sigma_1\sigma_2 + \sigma_2\sigma_3 + \sigma_1\sigma_3 = 1 + CK_p \tag{11b}$$

$$\sigma_1 + \sigma_2 + \sigma_3 = 2 - CK_p - CK_d \tag{11c}$$

or, after summing (11),

$$\sigma_1\sigma_2\sigma_3 + \sigma_1\sigma_2 + \sigma_2\sigma_3 + \sigma_1\sigma_3 + \sigma_1 + \sigma_2 + \sigma_3 = 3. \tag{12}$$

Substituting $1/\sigma_1 = x > 1$, $1/\sigma_2 = y > 1$, $1/\sigma_3 = v > 1$, (12) can be written as

$$v(x, y) = \frac{1 + x + y + xy}{3xy - x - y - 1}. \tag{13}$$

The minimization of $\mathcal{J}$ is equivalent to the maximization of $\mathcal{J}_1 = 1/\mathcal{J}$, which can be derived from (10–(13) as

$$\mathcal{J}_1 = x + y + v(x, y) - xyv(x, y). \tag{14}$$

The maximum of (14) can be obtained analytically to be for

$$x = y = v = \frac{1}{\sigma} = 1.702. \tag{15}$$

With optimal values (15), the characteristic polynomial of the closed-loop system becomes

$$f_1(z) = (z - \sigma)^3 = (z - 0.587)^3. \tag{16}$$

From (11a) and (11b), the optimal values of controller parameters are found to be

$$K_p = \frac{3\sigma^2 - 1}{C} = 0.03512/C \tag{17a}$$

$$K_d = \frac{\sigma^3}{C} = 0.2027/C. \tag{17b}$$

For the pertinent value of the parameter $C = 0.005$, and for corresponding values of controller parameters $K_p = 7.024$ and $K_d = 40.54$, the system in Fig. 1 was simulated, and the simulation results are given in Fig. 3. Evidently, the results are in agreement with expected aperiodical step responses.

B. PID Regulator for Position Control

In order to eliminate the steady-state position error in the presence of a constant or slowly varying torque disturbance $T_L(t)$, the system structure in Fig. 1 is modified by introducing the I action into the main control loop and replacing the P action from the main loop into the additional local control loop. In such a way and using the incremental version of the digital PID controller [7], the new system structure is obtained in the form shown in Fig. 4.

In the linear regime of operation, the closed-loop transfer functions from the inputs $\theta_r(t)$ and $T_L(t)$ to the output $\theta_0(t)$ of the system in Fig. 4 can be derived as follows:

$$\frac{\Theta_0(z)}{\Theta_r(z)} = W_\theta(z) = \frac{CK_i z^2(z+1)}{f_2(z)} \tag{18}$$

$$\frac{\Theta_0(z)}{T_L^*(z)} = W_t(z) = \frac{T^2}{2J}\frac{z(z^2-1)}{f_2(z)} \tag{19}$$

where parameter C is defined by (3), whereas $f_2(z)$ denotes the closed-loop system characteristic polynomial

$$\begin{aligned} f_2(z) = z^4 &+ (CK_i + CK_p + CK_d - 3)z^3 \\ &+ (CK_i - CK_d + 3)z^2 \\ &- (CK_p + CK_d + 1)z + CK_d. \end{aligned} \tag{20}$$

Now, the steady-state value of the output angle $\theta_0(t)$ may be calculated as

$$\begin{aligned} \theta_0(\infty) = \lim_{z\to 1}\{(1 - z^{-1})[&W_\theta(z)\theta_r/(1 - z^{-1}) \\ &- W_t(z)T_L/(1 - z^{-1})]\} = \theta_r. \end{aligned} \tag{21}$$

Hence, the steady-state position error, $e_{ss} = \theta_r(\infty) - \theta_0(\infty)$ is now equal to zero in the presence of both a constant input and a constant torque disturbance.

The procedure of adjusting controller parameters K_d, K_p, and K_i can be carried out in the same way as in the previous section. That is, the maximum speed of the aperiodical system step repsonse may be achieved by minimizing the

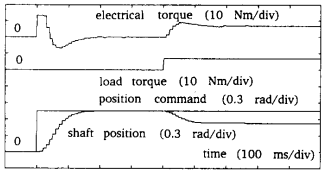

Fig. 3. Step responses of the torque and the shaft position in the servo with PD controller.

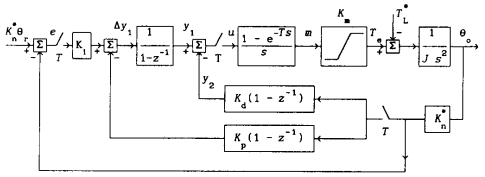

Fig. 4. Block diagram of the position servo with PID controller.

performance index (8). But, for the step input, now we have

$$E(z) = \frac{z[z^3 + (CK_p + CK_d - 2)z^2 + (1 + CK_p)z - CK_d]}{f_2(z)}\theta_r \tag{22}$$

and then

$$\mathcal{J} = E(z)\,|_{z=1} = \frac{CK_p}{CK_i}\theta_r = \frac{K_p}{K_i}\theta_r. \tag{23}$$

Hence, the optimal setting of the control parameters is reduced to the problem of determining the minimal value of K_p/K_i under the constraint that all zeros of closed-loop system characteristic polynomial (20) must lie on the positive part of the real axis inside the unit circle of the z plane. Let us suppose closed-loop system poles to be σ_1, σ_2, σ_3, and σ_4.

Introducing $x = 1/\sigma_1 > 1$, $y = 1/\sigma_2 > 1$, $v = 1/\sigma_3 > 1$, and $w = 1/\sigma_4 > 1$, performance index (23) can be written in the form

$$\mathcal{J} = \frac{x + y + v + w(x, y, v) - 1 - xyvw(x, y, v)}{1 + xy + yv + vw(x, y, v) + xv + yw(x, y, v) + xw(x, y, v) - 3xyvw(x, y, v)}\theta_r \tag{24}$$

where

$$w(x, y, v) = \frac{1 + x + y + v + xy + yv + xv + xyv}{7xyv - xy - yv - xv - x - y - v - 1}. \tag{25}$$

After substituting $w = w(x, y, v)$ from (25) into (24), the performance index $\mathcal{J}$ may be expressed in terms of three variables x, y, and v. The minimum of $\mathcal{J} = \mathcal{J}(x, y, v)$ in the region determined with $x > 1$, $y > 1$, $v > 1$, and $w > 1$ was analytically found to be for

$$x = y = v = w = 1.4666 \tag{26}$$

or

$$\sigma_1 = \sigma_2 = \sigma_3 = \sigma_4 = \sigma = 0.6818. \tag{27}$$

Thus, the characteristic polynomial of the closed-loop optimal system becomes

$$f_2(z) = (z - \sigma)^4 = (z - 0.6818)^4. \tag{28}$$

By equating identically corresponding coefficients of polynomials (20) and (28), and then solving the obtained identities for K_p, K_d, and K_i, one obtains

$$K_p = \frac{4\sigma^3 - 1 - \sigma^4}{C} = 0.051600/C \tag{29a}$$

$$K_d = \frac{\sigma^4}{C} = \frac{0.216000}{C} \tag{29b}$$

$$K_i = \frac{6\sigma^2 - 3 + \sigma^4}{C} = 0.005127/C. \tag{29c}$$

Fig. 5 shows the simulation results for the system in Fig. 4 with $C = 0.005$, and $K_p = 0.0516/C = 10.32$, $K_d = 0.216/C = 43.2$, and $K_i = 0.005127/C = 1.0254$. Notice that step responses are also aperiodical, but, in contrast to Fig. 3, now both components of the steady-state position error produced by a step input change and a constant torque disturbance are zero.

The comparison between the systems with PD and PID controllers is given in Table I. Notice that the PID control law eliminates the steady-state error completely, but it prolongs the settling time of the system step response approximately by the ratio of 1.5.

C. Nonlinear Control Laws

The control structures and the method of parameter setting proposed in Subsections A and B guarantee the optimal aperiodical system step response when the electrical torque of the motor does not reach limits imposed by the inverter current capacity. The positioning servomechanisms in Fig. 1 and 4 were simulated with a large position set point when the torque required by the linear controller cannot be actuated due to the bounded maximum torque ($|T_e| \le T_{max}$) of a real induction motor. Note that the step responses in Fig. 6 obtained in simulation runs are unacceptable because of large overshoots and long settling times.

In order to preserve aperiodical step responses as fast as possible even in the case when limits with respect to the available torque and/or allowable speed are reached, the nonlinear control laws must be introduced. This can be performed in two different ways. The solution that most control engineers are familiar with consists in reducing the slope of position reference and/or in limiting the reference

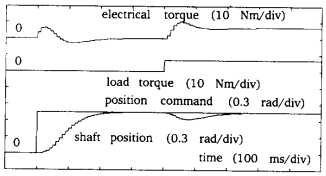

Fig. 5. Step responses of the torque and the shaft position in the servo with PID controller.

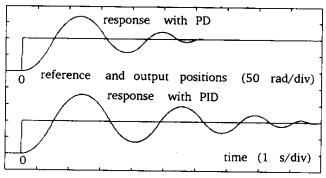

Fig. 6. Step responses of the shaft position in the case of a large position set point.

TABLE I
CHARACTERISTICS OF SERVOS WITH PD AND PID POSITION CONTROLLERS

Servo Characteristics	PD Controller	PID Controller
Optimal parameters	$K_p = 0.035120/C$ $K_d = 0.202700/C$	$K_d = 0.216000/C$ $K_p = 0.051600/C$ $K_i = 0.005127/C$
System order	3	4
Closed-loop poles	$z_{1,2,3} = 0.5870$	$z_{1,2,3,4} = 0.6818$
Settling times	$\approx 12T$	$\approx 18T$
Steady-state error caused by the load torque	$-\frac{T^2}{2CJK_p}T_{load}$	Zero

signal ω_r of the local speed control loop. In such a solution, the settling time of the resulting control system prolongs proportionally to the ratio between the rated and limited values of the motor speed.

Therefore, another solution referred to as a time-optimal position control with fixed target has been proposed [8], [9]. The solution is derived by calculus of variation and consists of two intervals of acceleration/deceleration and possibly an intermediate interval with constant maximum speed. The scheme differs from the linear one by the nonlinear function generating the speed reference ω_r as

$$\omega_r \sqrt{2a_{\max}|\theta_r - \theta_0|}\ \operatorname{sgn}(\theta_r - \theta_0) \tag{30}$$

where $a_{\max}$ represents the maximum acceleration, $a_{\max} = T_{\max}/J$.

The nonlinear control law (30) guides the drive with a constant maximum deceleration into the target point wherein the motor speed is reduced to zero. In the following, it will be shown how the time-optimal behavior [9] can be achieved by simple modifications of the PD and PID controllers, proposed in this paper.

To this end, let us suppose that the braking mode starts at the motor speed ω_p with maximum available braking torque $T_{\max}$. Then, the speed will be reduced to zero within the braking time interval

$$t_B = J\omega_p / T_{\max}. \tag{31}$$

The angular increment during the time interval t_B or the *braking distance* $\Delta\theta_B$ increases proportionally to the square of the speed ω_p, i.e.,

$$\Delta\theta_B(\omega_p) = t_B\omega_p/2 = J\omega_p^2/2T_{\max}. \tag{32}$$

Hence, to avoid the overshoot, the relation

$$|\Delta\theta| = |\theta_r - \theta_0| \geq \Delta\theta_B(\omega) \tag{33}$$

is to be held during the overall system response time. In virtue of (32), the relation (33) may be rewritten as the nonlinear constraint $\omega_c(\Delta\theta)$ determining the maximum allowable motor speed in terms of a position error

$$\omega_c(\Delta\theta) \leq \sqrt{\frac{2T_{\max}}{J}|\Delta\theta|}\ \operatorname{sgn}(\Delta\theta). \tag{34}$$

To introduce the nonlinear control law into the proposed PD and PID controllers, notice primarily that in both control structures in Figs. 1 and 4 the D action is located within the local minor loops. Then, let us consider the minor loop shown in Fig. 7 separately as a subsystem having the reference $y_1(kT)$ and feedback variable $y_2(kT)$. Notice, in the system with the PD controller (Fig. 1) that reference $y_1(kT)$ is generated by P action, whereas in the system with the PID controller (Fig. 4), the signal $y_1(kT)$ generate P and I action simultaneously. On the other hand, the velocity feedback y_2 is given by

$$y_2(z) = K_dK_n^*T\frac{z+1}{z}\omega(z) \tag{35}$$

where $\omega(z)$ denotes the z transform of the motor speed in radians per second. From (35), one may conclude that the subsystem in Fig. 7 can be considered as an autonomous speed regulator with proportional feedback and the speed reference $\omega_r = y_1/K_n^*K_dT$. To ensure the relation (33) (i.e., to avoid overshoots), the nonlinear function $\Omega(\Delta\theta)$ must be introduced in both PD and PID controllers, as a parabolic constraint for the signal y_1,

$$|y_1| \leq \Omega(\Delta\theta) = K_n^*K_dT\sqrt{\frac{2T\max}{J}|\theta_r - \theta_0|}. \tag{36}$$

The modification of the PD controller is performed simply by introducing the constraint (36) into the P action (see Fig. 8).

Fig. 9 visualizes the modified PID controller. Now, the reference signal $y_1(kT)$ appears as the output of the integral term. Therefore, to submit $y_1(kT)$ to constraint (36), the sum of the incremental input $\Delta y_1(kT)$ and past output value $y_1(kT - T)$ of the integral term is to be modified as illustrated in Fig. 9. In such a way, the modified PID controller comprises the D action unchanged, and the P and I actions constrained through an "intelligent integrator," which does not accumulate the so-called integration error when the controller output is saturated (see Fig. 9).

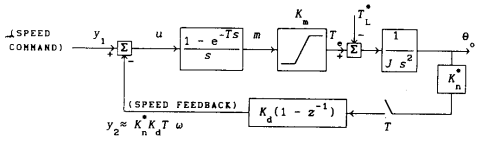

Fig. 7. Block diagram of the minor local loop.

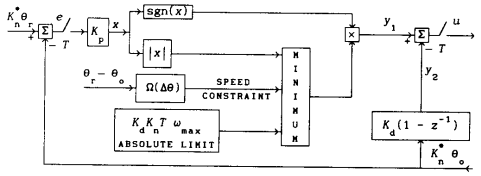

Fig. 8. Modification of PD controller.

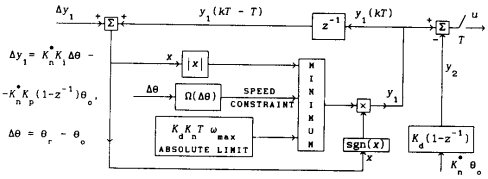

Fig. 9. Modification of the incremental version of PID controller.

For a large position set point, Fig. 10 shows the simulation results of the system with the modified PID controller. In Fig. 10, notice that the motor accelerates with the maximum available torque and then runs with the maximum allowable speed toward the target point while approaching the position target the motor brakes with the maximum available torque. Finally, the motor stops at the set position without overshoot. Simulation results (Fig. 10) and step responses obtained in an experimental setup (Figs. 15 and 16) show that the designed PD and PID controllers modified with suitable nonlinear control laws enable smooth transition from one mode of operation to another. Moreover, while approaching the desired position, the torque does not change sign—thus the backlash problem is considerably reduced. From a practical viewpoint, such control systems reveal more suitable characteristics when compared with systems designed to use strictly time-optimal switching control algorithms.

Control engineers often deal in practice with nonlinear control systems with magnitude constrained control variables. For example, in positioning servomechanisms, the slope of position reference and/or the magnitude of speed reference may be limited. Therefore, it is of interest to compare such a servomechanism with the one having the nonlinear position control suggested in this paper.

Let us consider the system with PD controller (Fig. 1). As mentioned, in order to avoid the overshoot in the system step response, the parabolic constraint (34) must be fulfilled during the overall system response time. The parabola obtained by equating left and right sides in (34) divides the ($|\Delta\theta|$, $|\omega_r|$) plain in two regions, corresponding to system step

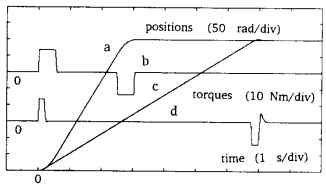

Fig. 10. Step response of the shaft position and torque in the case of a large position set point: (a), (b) for the system with modified PID controller; (c), (d) for the system with PID controller and magnitude-constrained speed reference.

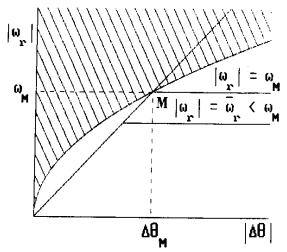

Fig. 11. Regions in the ($|\Delta\theta|$, $|\omega_r|$) plane corresponding to responses with and without overshoots.

responses with (shaded area) and without overshoots (unshaded area) (Fig. 11). In Fig. 11, the straight line

$$|\omega_r| = \frac{K_p}{K_d K_n^* T}|\Delta\theta| \tag{37}$$

corresponding to the linear control law $y_1 = K_p\Delta\theta$ was drawn.

The magnitude of speed reference $|\omega_r|$ may be limited on any value $\bar{\omega}_r$ inside the unshaded region in Fig. 11. But, to restrict the system operation to the unshaded side of parabola, the speed limit $\bar{\omega}_r$ may not exceed the value ω_M determined from the intersection (point M) of the straight line (37) and the parabola, as

$$\omega_M^{PD} = \frac{K_d}{K_p} K_n^* T \frac{2T_m}{J} \tag{38}$$

Actually, in the system with magnitude constrained speed reference, the condition $\bar{\omega}_r \le \omega_M$ is necessary but not sufficient for the step response without overshoot. That is, the condition implies that the settling time of the local minor speed control loop is negligible. Generally, it is not true and therefore a very small overshoot appears when $\bar{\omega}_r = \omega_M$ (see Figs. 10 and 12).

According to Fig. 11, for a small position set point, when $|\Delta\theta| \le \Delta\theta_M$ and $|\omega| \le \omega_M$, both the system suggested in this paper and the one having magnitude constrained speed reference work in the same linear regime and consequently, in this regime, their step responses are identical. For a large set point, when $|\Delta\theta|$ exceeds $\Delta\theta_M$, the system with magnitude constrained speed reference runs, during certain inter-

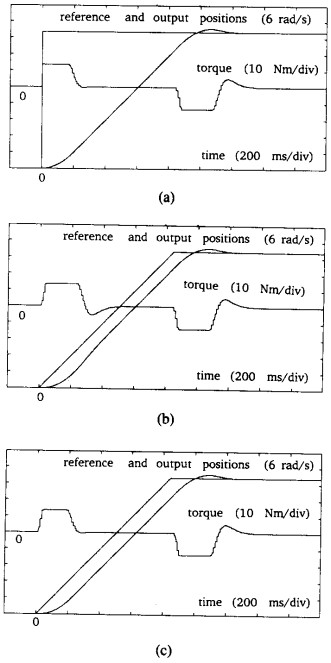

Fig. 12. Position references and responses of the output position and torque in the system with PID controller: (a) with magnitude constrained speed reference; (b) with bounded slope of position reference; (c) with both the magnitude constrained speed reference and bounded slope of position reference.

mediate interval, toward a desired position with the constant speed $\bar{\omega}_r$. On the other hand, when $|\Delta\theta| \geq \Delta\theta_M$, the system proposed in this paper runs toward the target position with the speed $\omega_c(\Delta\theta)$, which can be considerably greater than $\bar{\omega}_r$ (Figs. 10 and 11). For example, for the system with a PD controller the maximum allowable magnitude ω_M of speed reference is determined from (38) to be approximately 22% of the rated speed. Hence, the system with suggested nonlinear position control needs significantly shorter time interval to reach desired position without overshoot.

The similar discussion can be carried out in the case of the system with a PID controller (Fig. 4). In this system, the upper magnitude ω_M^{PID} of the speed reference is determined, after simple manipulations as in the case with PD controller, as

$$\omega_M^{\text{PID}} = \frac{K_p}{K_i} K_n^* T \frac{2T_m}{J}. \tag{39}$$

To demonstrate the advantage of the suggested nonlinear position control, two system with a PID controller were simulated: the first system with magnitude constrained speed reference $|\omega_r| \leq \omega_M^{\text{PID}}$, and the second one with ω_r subjected to the parabolic constraint (34). Simulation results are compared in Fig. 10. Both responses in Fig. 10 are aperiodical, but the system with suggested nonlinear position control requires remarkably shorter time interval to reach the desired position.

In order to avoid the overshoot, instead of limiting the magnitude of the speed reference, the slope of position reference may be bounded as $|d\theta_r/dt| \leq \omega_M$. Notice in Fig. 11 that the position error $|\Delta\theta|$ does not exceed $\Delta\theta_M$ and the system operates in the linear regime where $|\omega| \leq \omega_M$. The system with a PID controller was simulated with the magnitude constrained speed reference, with limited slope of the position reference, and with both limiters applied simultaneously. As it is expected, the obtained step responses are very similar. Notice in Fig. 12, with $\bar{\omega}_r = \omega_M$ or $|d\theta_r/dt| = \omega_M$, very small overshoots appear. As a conclusion, to ensure the aperiodical step response either magnitude of speed reference or the slope of position reference is to be limited; an application of both limiters is unnecessary.

III. Discussion

The prevailing problem that has to be solved in order to employ the induction motor as an actuator in the positioning servo is detection of the rotor flux Ψ_r. As is well known [1]–[3] for decoupled torque and flux control loops, both the magnitude and the spatial orientation of Ψ_r must be available. In position control applications, where low- and zero-speed operations are required, the rotor flux vector should be evaluated by means of the mathematical model of the rotor circuit having stator currents and the shaft position as inputs. The overall drive performance rely on the model accuracy; errors in evaluation of the rotor flux spatial orientation result in a coupling between the torque and flux loop, and in the oscillatory response [2]. Thus, the rotor circuit parameters appearing in the model must fit actual values of rotor winding parameters that depend mainly on the rotor temperature and level of magnetic saturation. A number of authors discussed the possibility for the on-line rotor resistance R_r identification [10]–[13], but proposed solutions are suitable for the R_r identification at the zero speed only in the cases where the load parameters are known [10] or when the torque pulsations caused by the test signal injection may be tolerated. A proposed adaptation mechanism (see Fig. 13) is intended to operate without the test signal injection and to track the R_r even at the zero speed. The mathematical model of the rotor circuit, shown in the block notation, calculates the rotor flux taking into account the magnetic nonlinearity; this circuit has been described in detail in [14]. Therefore, the motor's magnetizing characteristic is to be measured and stored in the microcontroller memory. Then, a thermal drift in the rotor resistance R_r is compensated on line by the adaptation mechanism and using the outputs of the rotor flux estimator.

The nonlinear rotor flux estimator gives the flux amplitude from terminal quantities so that the stator resistance voltage drop has no effect on an estimated value. This important feature guarantees the correct operation even at the zero speed of the motor shaft. The estimator output is then compared with the flux amplitude calculated in the model, and detected error is used as the reference for the adaptation

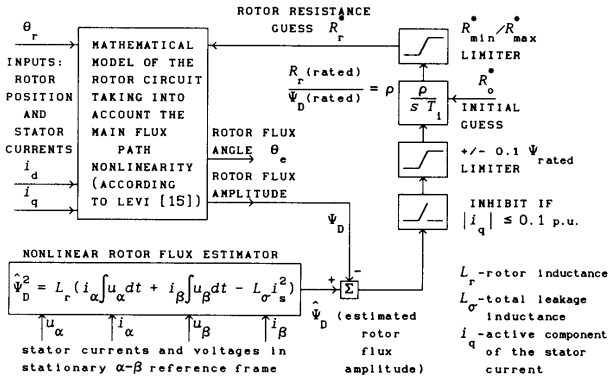

Fig. 13. Adaptation mechanism for tracking the changes in the rotor resistance R_r and updating the R_r^* parameter in the rotor circuit model.

mechanism, wherein the model parameter R_r^* is updated by the integral action. The integration time constant T_i determines the speed of convergence. The value of T_i must be large enough to suppress the interference between the adaptation process and the dynamic of the electrical subsystem. Since the sensitivity of the rotor flux amplitude with respect to a rotor resistance change drops to zero when the motor is unloaded ($i_q = 0$), the adaptation process is inhibited when $i_q < i_{q\,\min}$. For the motor under the test, temperature changes of the rotor resistance are compensated if the active component i_q periodically exceeds 10% of its rated value $i_{q\,\text{nom}}$. The rotor flux estimator and the adaptation mechanism are more evaluated in [6], and the results of experimental verification are given in the following section.

IV. Experimental Results

A real digitally controlled position servo was realized and tested. The motor was fed by a transistorized voltage-source inverter equipped with the specialized hardware for fast stator current control [6]. Relevant characteristics of the three-phase induction motor are nominal voltage 3 × 380 V, frequency 50 Hz, rotated speed 1410 rev/min, and output power 1 kW. The motor was loaded with the separately excited dc machine of 1.5 kW. The equivalent moment of inertia was measured as $J = 0.0459$ kg · m^2. Control structures, parameter settings, and interactive software were suited by the microcontroller system based on the Intel 8088/8087. For the detection of the motor speed and angular position, the incremental encoder giving 2500 pulses/rev was employed. With an adopted sampling period $T = 10$ ms, the plant parameter becomes $C = K_m K_n^* T^2/2J = 0.005$.

First, we tested the efficiency of the designed scheme for the rotor flux estimation and on-line compensation of temperature changes in the rotor resistance (see Fig. 13). In experiments, resistance change was simulated by the program. For nonzero speed, the resistance change ΔR compensates initially by a constant slope due to a limited $\Delta\Psi$ and the rotor resistance relatively quickly restores its correct value

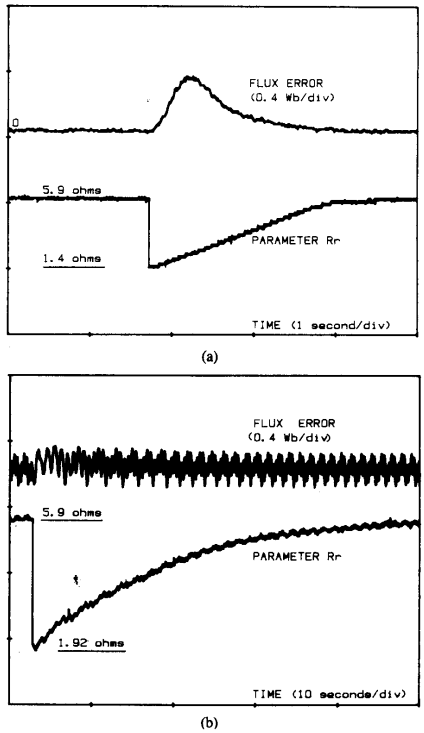

Fig. 14. Compensation of a change in the rotor resistance: (a) for $\omega \neq 0$; (b) for $\omega = 0$.

(Fig. 14(a)). For zero speed, the resistance change compensates more slowly than in the previous case (Fig. 14(b)) but is still sufficiently fast when compared with the slope of a motor temperature change. As a conclusion, the designed adaptation

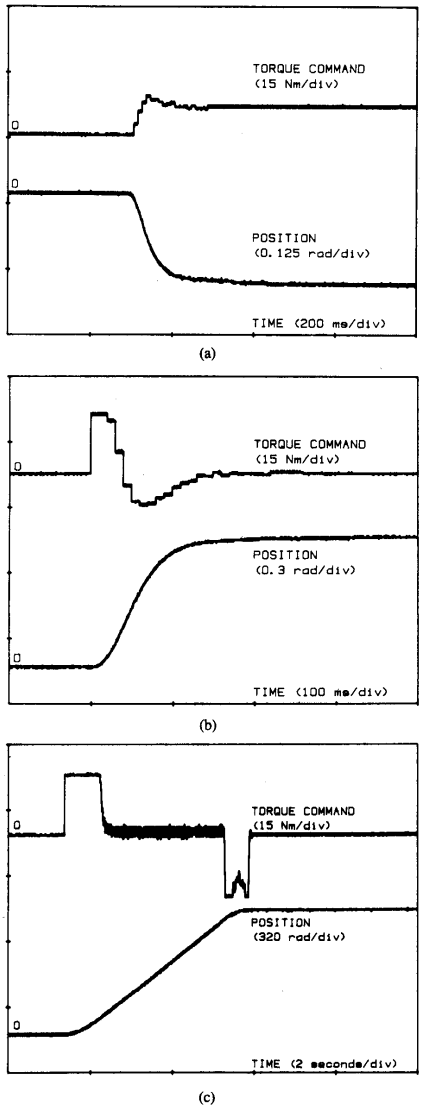

Fig. 15. Experimental waveforms measured on the servo with PD controller. Responses of the shaft position: (a) for a step load disturbance; (b) for the position set point of 0.1 revolution; (c) for the position set point of 96 revolutions.

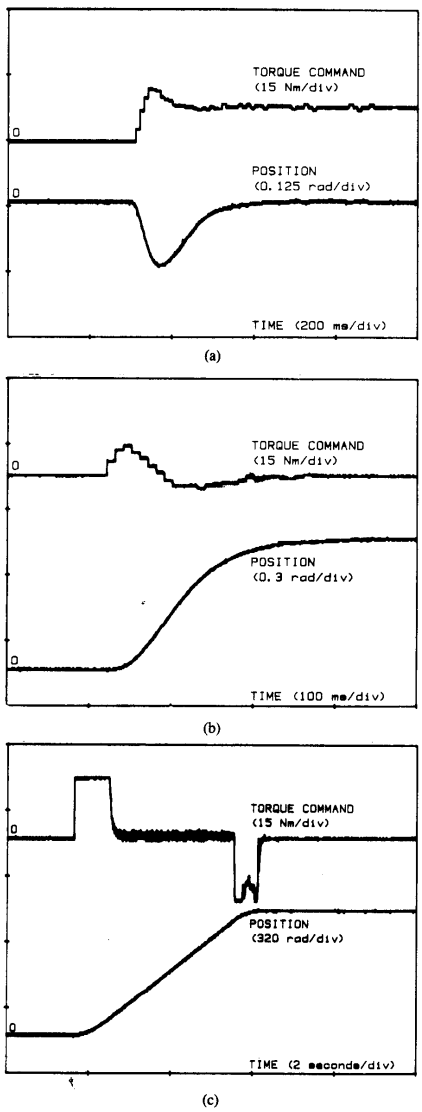

Fig. 16. Experimental waveforms measured on the servo with PID controller. Responses of the shaft position: (a) for a step load disturbance; (b) for the position set point of 0.1 revolution; (c) for the position set point of 96 revolutions.

mechanism can be advantageously applied to compensate changes of the motor resistance even at the zero shaft speed.

Figs. 15 and 16 illustrate the step responses of the shaft angle obtained in an experimental setup through the data acquisition/monitor system. We first investigated the performance of the position servo with a proposed PD controller for different position set points and load torque step disturbance. For the small position set point θ_r of only 0.1 revolution and for load torque step change of 6.8 Nm, the system operates within the linear regime (electrical torque does not saturate), and both step responses of the shaft angle, shown in Fig. 15(a) and (b), are aperiodical and optimal with

respect to performance index (8). Notice, in Fig. 15(b), that the steady-state position error due to a constant load torque disturbance exists. Fig. 15(c) shows the step response of the shaft angle in the case of the large position set point of 96 revolutions. Now, the system enters nonlinear modes of operation, wherein the designed nonlinear control laws activate. Notice in Fig. 15(c) that both the driving and braking electrical torques saturate; the motor initially accelerates with maximum available torque and then runs with maximum allowable speed; finally, it stops at the desired position without overshoot.

The same set of experiments was repeated to investigate the dynamic behavior of the proposed position servo with PID controller. Comparing the related responses in Figs. 15 and 16, one may conclude the following: (1) the aperiodical character of the step responses is preserved; (2) naturally, the introduction of the I action into the control law prolongs the system settling time; (3) the steady-state position error due to a constant load torque disturbance does not exist (see Fig. 16(a)).

The presented experimental results show that the proposed position servos operate in accordance with results of the analytical design developed in this paper. Moreover, in various operational conditions, introduced nonlinear control laws enable nearly time-optimal behavior with smooth transition from linear regime to nonlinear modes of operation.

V. Conclusions

Structures for a digitally controlled optimal position servo of induction motors have been proposed. The structures comprise combined (cascade and parallel) conventional PD and PID algorithms that most engineers are familiar with. The application of the proposed procedure for the setting of controller parameters gives optimal values of the P-, I-, and D-gain factors in terms of a single synthetic parameter, which can be easily measured on a real plant by a simple experiment. Appropriate nonlinear control laws were introduced to modify the optimal PD and PID controller in a way as to enable robust, nearly time optimal, reliable operation of a position servo for all possible magnitudes of the position set point. The suggested control structures, method of control parameter setting, and nonlinear control laws are of general interest; they can also be advantageously applied to the position-controlled dc motor drive.

An important problem of compensation of changes in the rotor resistance has been solved advantageously by the adaptation scheme designed to enable the compensation of resistance changes even at the zero shaft speed. This feature of the adaptation mechanism appears as a very important in the design of a position servo with induction motor.

Results of analytical design have been verified by simulation and then tested by experimental investigations of the real system. The simulation results and experimental data are in agreement, and the realized position servo runs very well in all operating conditions tested.

References

[1] F. Blaschke, "Das prinzip der feldorientierung die grundlage für die TRANSVEKTOR regelung von drehfeld-maschinen," *Siemens Zeitschrift*, vol. 45, no. 10, pp. 757-760, 1971.

[2] D. W. Novotny and R. D. Lorenz, "Introduction to field orientation and high performance AC drives," in *Publication Industrial Drives Committee IEEE Ind. Appl. Soc.*, 1985.

[3] R. Lessmeier and W. Leonhard, "Microprocessor controlled induction motor servo drive for high dynamic performance," in *Proc. Int. Conf. Evolution Modern Aspects Induction Machines* (Torino, Italy, July 8-11 1986), pp. 431-438.

[4] S. C. Lin and S. J. Tsai, "A microprocessor based incremental servo system with variable structure," *IEEE Trans. Ind. Electron.*, vol. IE-31, pp. 313-316, Nov. 1984.

[5] H. Haneda and A. Nagao, "Digitally controlled optimal position servo of induction motors," *IEEE Trans. Ind. Electron.*, vol. IE-36, pp. 349-360, Aug. 1989.

[6] S. Vukosavić, "Microprocessor-based adaptive speed and position control of induction motor drives," Ph.D. dissertation, Univ. of Belgrade, 1989 (in Serbocroatian).

[7] M. R. Stojić, *Digital Control Systems*. Belgrade: Scientific Book, 1989 (in Serbocroatian).

[8] W. Leonhard, *Control of Electrical Drives*. New York: Springer-verlag, 1985.

[9] A. J. Lerner, *Schnelligkeitsoptimale Regelungen*. Munich: Oldenbourg, 1963.

[10] K. Ohnishi, Y. Ueda, and K. Miyachi, "Model reference adaptive system against rotor resistance variations in induction motor drives," *IEEE Trans. Ind. Electron.*, vol. IE-33, pp. 217-223, Aug. 1986.

[11] L. Garces, "Parameter adaptation for the speed-controlled static AC-drive with squirrel-cage induction motor operated with variable frequency power supply," *IEEE Trans. Ind. Appl.*, vol. IA-16, pp. 173-178, Mar./Apr. 1980.

[12] H. Sugimoto and S. Tamai, "Secondary resistance identification of an induction motor applied model reference adaptive system and its characteristics," *IEEE Trans. Ind. Appl.*, vol. IA-23, pp. 296-303, Mar./Apr. 1987.

[13] R. D. Lorenz and D. B. Lawson, "A simplified approach to continuous on-line tuning of field oriented induction machine drives," in *Conf. Rec. IEEE Ind. Appl. Soc. Ann. Meet.*, 1988, pp. 444-449.

[14] E. Levi, S. Vukosavić and V. Vučković, "Saturation compensation schemes for vector controlled induction motor drives," in *Conf. Rec. 21st IEEE Power El. Spec. Conf. PESC'90*, 1990, pp. 591-598.